Analytic smearing of $SU(3)$ link variables in lattice QCD

Colin Morningstar
Department of Physics, Carnegie Mellon University, Pittsburgh, Pennsylvania 15213, USA

Mike Peardon
School of Mathematics, Trinity College, Dublin 2, Ireland
(Received 11 November 2003; published 23 March 2004)

An analytic method of smearing link variables in lattice QCD is proposed and tested. The differentiability of the smearing scheme with respect to the link variables permits the use of modern Monte Carlo updating methods based on molecular dynamics evolution for gauge-field actions constructed using such smeared links. In examining the smeared mean plaquette and the static quark-antiquark potential, no degradation in effectiveness is observed as compared to link smearing methods currently in use, although an increased sensitivity to the smearing parameter is found.

DOI: 10.1103/PhysRevD.69.054501 PACS number(s): 12.38.Gc, 11.15.Ha, 12.39.Mk

I. INTRODUCTION

The extraction of hadron masses and matrix elements from Monte Carlo estimates of Euclidean-space correlation functions in lattice QCD can be done more reliably and accurately when operators which couple more strongly to the states of interest and less strongly to the higher-lying contaminating states are used. For states containing gluons, a crucial ingredient in constructing such operators in lattice QCD is link variable smearing. Operators constructed out of smeared or fuzzed links have dramatically reduced mixings with the high frequency modes of the theory. The use of such operators has been shown to especially benefit determinations of the glueball spectrum [1], hybrid meson masses [2,3], the torelon spectrum [4], and excitations of the static quark-antiquark potential [5].

Link variable smoothing is also playing an increasingly important role in the construction of improved lattice actions. In Ref. [6], the use of so-called fat links in a staggered quark action was shown to significantly decrease flavor symmetry breaking. Smeared links were subsequently used [7] to construct hypercubic fermion actions having improved rotational invariance. A staggered fermion action using a link smearing transformation [8] known as hypercubic (HYP) fat links was shown to improve flavor symmetry by an order of magnitude relative to the standard action. The so-called Asqtad improved staggered quark action [9–11] also makes use of link fattening to reduce flavor symmetry breaking. Another variant of fermion actions which exploit smeared link variables is the fat link irrelevant clover (FLIC) action [12]. FLIC fermions are Wilson-like and described by an action which includes an irrelevant clover improvement term constructed using smeared links. Fat links have also been used to construct a gauge action [13] with reduced discretization errors using approximate renormalization group transformations.

The link fuzzing algorithm most often used in gluonic operator construction is that described in Ref. [14] in which every spatial link $U_j(x)$ on the lattice is replaced by itself plus a real weight ρ times the sum of its four neighboring (spatial) staples, projected back into $SU(3)$. Such a fuzzing step is iterated n_ρ times to obtain the final fuzzed link variables. Empirically, one finds that the projection into $SU(3)$ is a crucial ingredient of the smearing. Link smearings which do not apply such a projection are found to be much less effective. The projection into $SU(3)$ is not unique and must be carefully defined so that all symmetry properties of the link variables are preserved. Various ways of implementing this projection have appeared in the literature. Given a 3×3 matrix V, its projection U into $SU(3)$ is often taken to be the matrix $U\in SU(3)$ which maximizes $\mathrm{Re\,Tr}(UV^\dagger)$. An iterative procedure is required to perform such a maximization. Alternatively [15], the projected matrix U can be defined by $U=V(V^\dagger V)^{-1/2}\det(V^{-1}V^\dagger)^{1/6}$.

Although the above smearing procedure works well in practice, the projection is somewhat unpalatable since it may be viewed as an arbitrary and abrupt way to remain within the group. More importantly, the branch cuts and lack of differentiability inherent in the projection can hinder or even make impossible the application of modern Monte Carlo updating techniques, such as the hybrid Monte Carlo (HMC) [16] algorithm, which require knowing the response of the action to a small change in one of the link variables.

A link smearing method which circumvents these problems is proposed and tested in this paper. The link smearing method is analytic everywhere in the finite complex plane and utilizes the exponential function in such a manner to remain within $SU(3)$, eliminating the need for any projection back into the group. Because of this construction, the algorithm is useful for any Lie group. The method is described in Sec. II and its practical implementations when constructing operators and when computing the response of the action to a change in a link variable are detailed in Secs. III and IV, respectively. Numerical tests of the smearing are presented in Sec. V. Using the smeared plaquette and the effective mass $aE_{\mathrm{eff}}(t)$ associated with the static quark-antiquark potential, no degradation in effectiveness is observed as compared to the standard link smearing method, although an increased sensitivity to the smearing parameter is found. The results also suggest that lattice actions and operators constructed out of smeared link variables may be much less afflicted by radiative corrections since the usually-dominant large tadpole contributions are drastically reduced.

 ©2004 The American Physical Society

II. ANALYTIC LINK SMEARING

A method of smearing link variables which is analytic, and hence differentiable, everywhere in the finite complex plane can be defined as follows. Let $C_\mu(x)$ denote the weighted sum of the perpendicular staples which begin at lattice site x and terminate at neighboring site $x+\hat{\mu}$:

$$C_\mu(x)=\sum_{\nu\neq\mu}\rho_{\mu\nu}(U_\nu(x)U_\mu(x+\hat{\nu})U_\nu^\dagger(x+\hat{\mu}) + U_\nu^\dagger(x-\hat{\nu})U_\mu(x-\hat{\nu})U_\nu(x-\hat{\nu}+\hat{\mu})), \quad (1)$$

where $\hat{\mu},\hat{\nu}$ are vectors in directions μ,ν, respectively, having the length of one lattice spacing in that direction (fundamental lattice translation vectors). The weights $\rho_{\mu\nu}$ are tunable real parameters. Then the matrix $Q_\mu(x)$, defined in $SU(N)$ by

$$Q_\mu(x)=\frac{i}{2}(\Omega_\mu^\dagger(x)-\Omega_\mu(x))-\frac{i}{2N}\mathrm{Tr}(\Omega_\mu^\dagger(x)-\Omega_\mu(x)),$$

$$\Omega_\mu(x)=C_\mu(x)U_\mu^\dagger(x) \quad \text{(no summation over } \mu) \quad (2)$$

is Hermitian and traceless, and hence, $e^{iQ_\mu(x)}$ is an element of $SU(N)$. We use this fact to define an iterative, analytic link smearing algorithm in which the links $U_\mu^{(n)}(x)$ at step n are mapped into links $U_\mu^{(n+1)}(x)$ using

$$U_\mu^{(n+1)}(x)=\exp(iQ_\mu^{(n)}(x))\,U_\mu^{(n)}(x). \quad (3)$$

The fact that $e^{iQ_\mu(x)}$ is an element of $SU(N)$ guarantees that $U_\mu^{(n+1)}(x)$ is also an element of $SU(N)$, eliminating the need for a projection back onto the gauge group. This fuzzing step can be iterated n_ρ times to finally produce link variables which we call *stout links* [17], denoted by $\tilde{U}_\mu(x)$:

$$U\to U^{(1)}\to U^{(2)}\to\cdots\to U^{(n_\rho)}\equiv\tilde{U}. \quad (4)$$

One common choice of the staple weights is

$$\rho_{jk}=\rho, \quad \rho_{4\mu}=\rho_{\mu4}=0, \quad (5)$$

which yields a three-dimensional scheme in which only the spatial links are smeared. Another common choice is an isotropic four-dimensional scheme in which all weights are chosen to be the same $\rho_{\mu\nu}=\rho$. Note that such a scheme was used in Ref. [18] as a field transformation to eliminate a certain interaction term from the most general $O(a^2)$ on-shell improved gauge action.

It is not difficult to show that, given an appropriate choice of weights $\rho_{\mu\nu}$, the stout links have symmetry transformation properties identical to those of the original link variables. Under any local gauge transformation $G(x)$, the link variables transform as $U_\mu(x)\to G(x)U_\mu(x)G^\dagger(x+\hat{\mu})$, where the $G(x)$ are $SU(N)$ matrices. Thus, under such a gauge transformation,

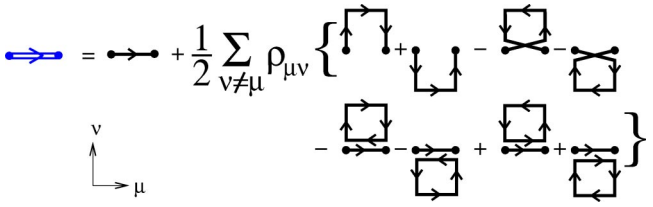

FIG. 1. The expansion up to first order in the $\rho_{\mu\nu}$ of the new link variable $U^{(1)}$ in terms of paths of the original links. Each closed loop includes a trace with a factor $1/N$ in $SU(N)$. In the third and fourth terms inside the brace brackets above, the crossed lines indicate a traversal of the same link in opposite directions.

$$Q_\mu(x)\to G(x)Q_\mu(x)G^\dagger(x), \quad (6)$$

$$e^{iQ_\mu(x)}\to G(x)e^{iQ_\mu(x)}\;G^\dagger(x), \quad (7)$$

$$U_\mu^{(1)}(x)\to G(x)e^{iQ_\mu(x)}G^\dagger(x)G(x)U_\mu(x)G^\dagger(x+\hat{\mu}) = G(x)U_\mu^{(1)}(x)G^\dagger(x+\hat{\mu}), \quad (8)$$

as required. One can also easily show that if the weights $\rho_{\mu\nu}$ respect the rotation and reflection symmetries of the lattice, the stout links obey the required transformation properties under all rotations and all reflections in a plane containing the link. Lastly, consider a reflection in a plane normal to a link $U_\mu(x)$ and passing through its midpoint $x+\frac{1}{2}\hat{\mu}$. Under such an operation, the link $U_\mu(x)$ transforms according to $U_\mu(x)\to U_{-\mu}(x+\hat{\mu})=U_\mu^\dagger(x)$ and for the case $\nu\neq\mu$, $U_\nu(x)\leftrightarrow U_\nu(x+\hat{\mu})$ and $U_\nu^\dagger(x+\hat{\mu})\leftrightarrow U_\nu^\dagger(x)$, yielding $C_\mu(x)\to C_\mu^\dagger(x)$ assuming the $\rho_{\mu\nu}$ are real, so that

$$\Omega_\mu(x)\to C_\mu^\dagger(x)U_\mu(x)=U_\mu^\dagger(x)\Omega_\mu^\dagger(x)U_\mu(x), \quad (9)$$

$$Q_\mu(x)\to -U_\mu^\dagger(x)Q_\mu(x)U_\mu(x), \quad (10)$$

$$U_\mu^{(1)}(x)\to U_\mu^\dagger(x)e^{-iQ_\mu(x)}=U_\mu^{(1)\dagger}(x), \quad (11)$$

as required. Given that $U_\mu^{(1)}(x)$ transforms under all symmetry operations in the same manner as $U_\mu(x)$, it follows that the stout links $\tilde{U}_\mu(x)$ have symmetry transformation properties identical to those of the original link variables.

Since the exponential function has a power series expansion with an infinite radius of convergence, each stout link may be viewed as an incredibly large and complicated sum of paths. For small $\rho_{\mu\nu}$, the paths which make up the link variable $U^{(1)}$ to first order in the $\rho_{\mu\nu}$ are shown in Fig. 1. Note that the standard smearing method, defined by

$$U_\mu^{(1)}(x)=\mathcal{P}_{SU(3)}\{U_\mu(x)+C_\mu(x)\}, \quad (12)$$

where $\mathcal{P}_{SU(3)}$ denotes the projection into $SU(3)$, yields the same sum of paths at first order in $\rho_{\mu\nu}$.

A few further remarks are worthy of note. First, an alternative smearing scheme in which the weights $\rho_{\mu\nu}$ are chosen to be imaginary does not reduce the couplings to the high-frequency modes of the theory. Secondly, it is not possible to remove the leading $O(a^2)$ discretization errors in the Wilson

gauge action by expressing the action in terms of stout links; diminishing the $O(\alpha_s a^2)$ errors by reducing their tadpole contributions is the best which can be achieved. Thirdly, the use of stout links in Symanzik-improved actions may eliminate the need to use tadpole-improvement in determining the couplings in the action. Lastly, the definition of $C_\mu(x)$ given in Eq. (1) is not unique. Analytic smearing schemes can be constructed as outlined above using sums of other paths from site x to $x+\hat{\mu}$, such as those used in fat link [6] and HYP [8] smearings.

III. IMPLEMENTATION OF THE SMEARING

To implement this analytic link smearing scheme, the efficient evaluation of $\exp(iQ)$, where Q is a traceless Hermitian 3×3 matrix, is required. The Cayley-Hamilton theorem states that every matrix is a zero of its characteristic polynomial, so that

$$Q^3 - c_1 Q - c_0 I = 0, \tag{13}$$

where

$$c_0 = \det Q = \tfrac{1}{3}\,\mathrm{Tr}(Q^3), \tag{14}$$

$$c_1 = \tfrac{1}{2}\,\mathrm{Tr}(Q^2) \geqslant 0. \tag{15}$$

The Hermiticity of Q requires $27c_0^2 - 4c_1^3 \leqslant 0$ and the definition of Q given in Eq. (2) restricts the possible values of c_1. Thus, the coefficients c_0 and c_1 satisfy

$$-c_0^{\max} \leqslant c_0 \leqslant c_0^{\max}, \quad 0 \leqslant c_1 \leqslant c_1^{\max}, \tag{16}$$

where

$$c_0^{\max} = 2\left(\frac{c_1}{3}\right)^{3/2}, \tag{17}$$

$$c_1^{\max} = \frac{1}{32}(69+11\sqrt{33})\left(\sum_{\nu\neq\mu}\rho_{\mu\nu}\right)^2, \tag{18}$$

for each μ. Equation (13) implies that Q^n for integer $n \geqslant 3$ can be expressed in terms of Q^2, Q, and the identity matrix I. Hence, we can write

$$e^{iQ} = f_0 I + f_1 Q + f_2 Q^2, \tag{19}$$

where the three scalar coefficients $f_j = f_j(c_0, c_1)$ are basis independent, depending only on c_0 and c_1. Equation (19) is valid for *any* 3×3 Hermitian, traceless matrix Q.

Let q_1, q_2, q_3 denote the three eigenvalues of Q. Since Q is Hermitian and traceless, we know that these are real numbers satisfying $q_1+q_2+q_3=0$. These eigenvalues are the three roots of a cubic polynomial which can be easily determined:

$$q_1 = 2u, \tag{20}$$

$$q_2 = -u + w, \tag{21}$$

$$q_3 = -q_1 - q_2 = -u - w, \tag{22}$$

where

$$u = \sqrt{\frac{1}{3}c_1}\cos\left(\frac{1}{3}\theta\right), \tag{23}$$

$$w = \sqrt{c_1}\sin\left(\frac{1}{3}\theta\right), \tag{24}$$

$$\theta = \arccos\left(\frac{c_0}{c_0^{\max}}\right). \tag{25}$$

Given these eigenvalues, the matrix Q can be written

$$Q = M\Lambda_Q M^{-1}, \quad \Lambda_Q = \begin{bmatrix} q_1 & 0 & 0 \\ 0 & q_2 & 0 \\ 0 & 0 & q_3 \end{bmatrix}, \tag{26}$$

where M is a unitary matrix. Then it easily follows that

$$e^{i\Lambda_Q} = f_0 I + f_1 \Lambda_Q + f_2 \Lambda_Q^2. \tag{27}$$

Explicitly, we have the following linear system of equations to solve:

$$\begin{bmatrix} 1 & q_1 & q_1^2 \\ 1 & q_2 & q_2^2 \\ 1 & q_3 & q_3^2 \end{bmatrix}\begin{bmatrix} f_0 \\ f_1 \\ f_2 \end{bmatrix} = \begin{bmatrix} e^{iq_1} \\ e^{iq_2} \\ e^{iq_3} \end{bmatrix}. \tag{28}$$

If all three eigenvalues are distinct, this system of equations has a unique solution, but when two of the eigenvalues are exactly the same, the solution to Eq. (28) is not unique and one of the f_j's can be freely set to any value. The case of degenerate eigenvalues occurs when $c_0 \to \pm c_0^{\max}$.

In practice, it is extremely unlikely that an exact degeneracy will be encountered during a numerical simulation. Much more likely is the possibility that two eigenvalues are nearly, but not quite, equal. Encounters with both near and exact degeneracies can be handled by expressing the f_j in terms of u and w in order to isolate and tame the numerically sensitive part. One finds that the f_j factors can be written

$$f_j = \frac{h_j}{(9u^2 - w^2)}, \tag{29}$$

where the h_j are well-behaved functions given by

$$h_0 = (u^2 - w^2)e^{2iu} + e^{-iu}\{8u^2\cos(w) + 2iu(3u^2 + w^2)\xi_0(w)\}, \tag{30}$$

$$h_1 = 2ue^{2iu} - e^{-iu}\{2u\cos(w) - i(3u^2 - w^2)\xi_0(w)\}, \tag{31}$$

$$h_2 = e^{2iu} - e^{-iu}\{\cos(w) + 3iu\xi_0(w)\}, \tag{32}$$

defining

$$\xi_0(w) = \frac{\sin w}{w}. \tag{33}$$

The $w \to 0$ problem as $c_0 \to c_0^{\max}$ has been completely contained in ξ_0. To numerically evaluate this factor, one uses, for example,

$$\xi_0(w) = \begin{cases} 1 - \frac{1}{6}w^2(1 - \frac{1}{20}w^2(1 - \frac{1}{42}w^2)), & |w| \leqslant 0.05, \\ \sin(w)/w, & |w| > 0.05. \end{cases}$$

However, the $w \to 3u \to \sqrt{3}/2$ limit as $c_0 \to -c_0^{\max}$ has not been tamed. Fortunately, this problem can be circumvented using the following symmetry relations under $c_0 \to -c_0$:

$$f_j(-c_0, c_1) = (-)^j f_j^*(c_0, c_1). \tag{34}$$

Thus, the determination of the f_j coefficients for $c_0 < 0$ can be achieved by computing the coefficients for $|c_0|$ and utilizing Eq. (34). This means that a situation in which the denominator in Eq. (29) becomes nearly zero will never be encountered. It should be emphasized that the f_j coefficients are smooth, nonsingular functions of c_0 and c_1. There are no actual singularities as $c_0 \to \pm c_0^{\max}$. The numerical evaluation of the f_j coefficients to machine precision in these limits simply requires additional care.

As an aside, if one writes $Q = \frac{1}{2}\sum_{a=1}^{8} Q_a \lambda^a$ in terms of the eight Gell-Mann matrices λ^a, then

$$e^{iQ} = u_0 + \frac{1}{2}\sum_{a=1}^{8} u_a \lambda^a, \tag{35}$$

$$u_0 = f_0 + \frac{2}{3} c_1 f_2, \tag{36}$$

$$u_a = f_1 Q_a + \frac{1}{2} f_2 d^{abc} Q_b Q_c, \tag{37}$$

$$c_0 = \frac{1}{12} d^{abc} Q_a Q_b Q_c, \tag{38}$$

$$c_1 = \frac{1}{4} Q_a Q_a, \tag{39}$$

where d^{abc} and f^{abc} are the real symmetric and antisymmetric structure constants, respectively.

IV. MOLECULAR DYNAMICS EVOLUTION

The analyticity of the stout-link scheme permits the use of modern Monte Carlo updating methods for gauge-field actions constructed using stout links. Molecular dynamics evolution forms the core of many of the Markov processes used to generate ensembles of field configurations needed for unquenched QCD simulations [16,19–21]. Since a small change to the underlying gauge fields always leads to a small change in the stout links, then provided the small change to the stout links causes small changes to the action of the theory, the force term on the underlying links is always well-defined. The importance of defining a link smearing scheme which permits the computation of the molecular dynamics force term has been emphasized recently in Ref. [22].

The $\Sigma_\mu(x)$ force field describes how the action S changes when the gauge-field link variables $U_\mu(x)$ change, holding the momenta $P_\mu(x)$ and the pseudofermion field $\phi(x)$ fixed. For this reason, we shall write the action $S = S[U]$ in this section, ignoring its dependence on the pseudofermion field. The transpose of the force field is defined by the derivative of the action with respect to the link variables in a component-wise manner:

$$\Sigma_\mu^{ab}(x) \equiv \frac{\partial S[U]}{\partial U_\mu^{ba}(x)}. \tag{40}$$

Assume that the action can be written as a sum of a term $S_{\rm th}[U]$ constructed entirely of the original thin link variables and a term $S_{\rm st}[\tilde{U}]$ constructed completely out of stout links:

$$S[U] = S_{\rm th}[U] + S_{\rm st}[\tilde{U}]. \tag{41}$$

Then the force field may be written

$$\Sigma_\mu(x) = \Sigma_\mu^{(\rm th)}(x) + \Sigma_\mu^{(0)}(x), \tag{42}$$

where

$$\Sigma_\mu^{(\rm th)}(x) = \left(\frac{\partial S_{\rm th}[U]}{\partial U_\mu(x)}\right)^T, \quad \Sigma_\mu^{(0)}(x) = \left(\frac{\partial S_{\rm st}[\tilde{U}]}{\partial U_\mu(x)}\right)^T. \tag{43}$$

The computation of $\Sigma_\mu^{(\rm th)}(x)$ is usually straightforward, and nothing more about its determination needs discussion here. We now focus on the evaluation of $\Sigma_\mu^{(0)}(x)$.

Recall that the stout links are constructed iteratively starting with the original links $U \to U^{(1)} \to U^{(2)} \to \cdots \to U^{(n_\rho)} = \tilde{U}$. The computation of the force field proceeds similarly in an iterative fashion, except that the order is reversed $\tilde{\Sigma} = \Sigma^{(n_\rho)} \to \Sigma^{(n_\rho - 1)} \to \cdots \to \Sigma^{(1)} \to \Sigma^{(0)}$. The sequence starts by computing

$$\tilde{\Sigma}_\mu(x) = \left(\frac{\partial S_{\rm st}[\tilde{U}]}{\partial \tilde{U}_\mu(x)}\right)^T. \tag{44}$$

This step depends on the form of the gauge and fermion action in terms of the stout links and is usually just as straightforward as the computation of $\Sigma_\mu^{(\rm th)}(x)$. In subsequent steps, $\Sigma^{(k)}$ and $U^{(k-1)}$ are used to compute $\Sigma^{(k-1)}$, where the effective force at level k is defined by

$$\Sigma_\mu^{(k)}(x) = \left(\frac{\partial S_{\rm st}[\tilde{U}]}{\partial U_\mu^{(k)}(x)}\right)^T. \tag{45}$$

The recursive mapping

$$\{\Sigma^{(k)}, U^{(k-1)}\} \to \Sigma^{(k-1)} \tag{46}$$

is repeated until $\Sigma^{(0)}$ is finally evaluated.

In Monte Carlo methods based on molecular dynamics, such as HMC [16] and the *R*-algorithm [21], the flow of lattice configurations through phase space via Hamilton's equations is parametrized by a fictitious simulation time coordinate τ. To determine the mapping in Eq. (46), it is convenient to express the force field in terms of the rate of change of the action with respect to this time coordinate τ:

$$\frac{d}{d\tau}S_{\rm st}[\tilde{U}]=2\sum_{x,\mu}\ {\rm Re\,Tr}\left\{\Sigma_\mu^{(k)}(x)\frac{d}{d\tau}U_\mu^{(k)}(x)\right\}, \qquad (47)$$

for $k=0,1,\ldots,n_\rho$ and defining $dU/d\tau$ in a component-wise manner. One then proceeds using the chain rule of differentiation:

$$\frac{dU_\mu^{(k)}(x)}{d\tau}=e^{iQ_\mu^{(k-1)}(x)}\frac{dU_\mu^{(k-1)}(x)}{d\tau} + \frac{d(e^{iQ_\mu^{(k-1)}(x)})}{d\tau}U_\mu^{(k-1)}(x). \qquad (48)$$

To simplify matters, $Q_\mu^{(k-1)}(x)$, $U_\mu^{(k-1)}(x)$, $\Sigma_\mu^{(k-1)}(x)$ shall simply be written as Q,U,Σ, respectively, in the calculations which follow, and $\Sigma_\mu^{(k)}(x)$ and $U_\mu^{(k)}(x)$ shall be written as Σ' and U', respectively. The Cayley-Hamilton theorem gives us

$$\frac{d(e^{iQ})}{d\tau}=\frac{d}{d\tau}(f_0+f_1Q+f_2Q^2),$$
$$=\frac{df_0}{d\tau}+\frac{df_1}{d\tau}Q+\frac{df_2}{d\tau}Q^2+f_1\frac{dQ}{d\tau} + f_2\frac{dQ}{d\tau}Q+f_2Q\frac{dQ}{d\tau}. \qquad (49)$$

Since the f_j coefficients are functions $f_j=f_j(u,w)$ of u and w only, one has

$$\frac{df_j}{d\tau}=\left(\frac{\partial f_j}{\partial u}\right)\frac{du}{d\tau}+\left(\frac{\partial f_j}{\partial w}\right)\frac{dw}{d\tau}, \qquad (50)$$

and since u and w are functions of c_0 and c_1 only, then

$$\frac{du}{d\tau}=\left(\frac{\partial u}{\partial c_0}\right)\frac{dc_0}{d\tau}+\left(\frac{\partial u}{\partial c_1}\right)\frac{dc_1}{d\tau}, \qquad (51)$$

$$\frac{dw}{d\tau}=\left(\frac{\partial w}{\partial c_0}\right)\frac{dc_0}{d\tau}+\left(\frac{\partial w}{\partial c_1}\right)\frac{dc_1}{d\tau}. \qquad (52)$$

Next, one finds that

$$\frac{dc_0}{d\tau}=\frac{1}{3}\frac{d}{d\tau}{\rm Tr}(Q^3)={\rm Tr}\left(Q^2\frac{dQ}{d\tau}\right), \qquad (53)$$

$$\frac{dc_1}{d\tau}=\frac{1}{2}\frac{d}{d\tau}{\rm Tr}(Q^2)={\rm Tr}\left(Q\frac{dQ}{d\tau}\right), \qquad (54)$$

and

$$\frac{\partial u}{\partial c_0}=\frac{1}{2(9u^2-w^2)}, \quad \frac{\partial u}{\partial c_1}=\frac{u}{(9u^2-w^2)},$$
$$\frac{\partial w}{\partial c_0}=\frac{-3u}{2w(9u^2-w^2)}, \quad \frac{\partial w}{\partial c_1}=\frac{3u^2-w^2}{2w(9u^2-w^2)}. \qquad (55)$$

Now define

$$r_j^{(1)}=\frac{\partial h_j}{\partial u}, \quad r_j^{(2)}=\frac{1}{w}\frac{\partial h_j}{\partial w}, \qquad (56)$$

and

$$b_{1j}=\frac{2ur_j^{(1)}+(3u^2-w^2)r_j^{(2)}-2(15u^2+w^2)f_j}{2(9u^2-w^2)^2}, \qquad (57)$$

$$b_{2j}=\frac{r_j^{(1)}-3ur_j^{(2)}-24uf_j}{2(9u^2-w^2)^2}. \qquad (58)$$

Then

$$\frac{df_j}{d\tau}=b_{1j}{\rm Tr}\left(Q\frac{dQ}{d\tau}\right)+b_{2j}{\rm Tr}\left(Q^2\frac{dQ}{d\tau}\right), \qquad (59)$$

where

$$r_0^{(1)}=2(u+i(u^2-w^2))e^{2iu}+2e^{-iu}\{4u(2-iu)\cos w + i(9u^2+w^2-iu(3u^2+w^2))\xi_0(w)\}, \qquad (60)$$

$$r_1^{(1)}=2(1+2iu)e^{2iu}+e^{-iu}\{-2(1-iu)\cos w + i(6u+i(w^2-3u^2))\xi_0(w)\}, \qquad (61)$$

$$r_2^{(1)}=2ie^{2iu}+ie^{-iu}\{\cos w-3(1-iu)\xi_0(w)\}, \qquad (62)$$

$$r_0^{(2)}=-2e^{2iu}+2iue^{-iu}\{\cos w+(1+4iu)\xi_0(w) + 3u^2\xi_1(w)\}, \qquad (63)$$

$$r_1^{(2)}=-ie^{-iu}\{\cos w+(1+2iu)\xi_0(w)-3u^2\xi_1(w)\}, \qquad (64)$$

$$r_2^{(2)}=e^{-iu}\{\xi_0(w)-3iu\xi_1(w)\}, \qquad (65)$$

with

$$\xi_0(w)=\frac{\sin w}{w}, \qquad (66)$$

$$\xi_1(w)=\frac{\cos w}{w^2}-\frac{\sin w}{w^3}. \qquad (67)$$

Given the above results,

$$\frac{d(e^{iQ})}{d\tau} = \mathrm{Tr}\left(Q\frac{dQ}{d\tau}\right) B_1 + \mathrm{Tr}\left(Q^2\frac{dQ}{d\tau}\right) B_2 + f_1\frac{dQ}{d\tau} + f_2\frac{dQ}{d\tau}Q + f_2 Q\frac{dQ}{d\tau}, \tag{68}$$

where

$$B_i = b_{i0} + b_{i1}Q + b_{i2}Q^2. \tag{69}$$

The numerically sensitive $w\to 0$ limit has been totally absorbed into ξ_0 and ξ_1, and numerical problems as $c_0 \to -c_0^{\max}$ can be circumvented by exploiting the following symmetry relation:

$$b_{ij}(-c_0, c_1) = (-)^{i+j+1} b_{ij}^*(c_0, c_1). \tag{70}$$

Once again, we emphasize that these coefficients are well-behaved, nonsingular functions of c_0 and c_1.

The rate of change of the stout links with respect to the simulation time is then given by

$$\frac{dU'}{d\tau} = e^{iQ}\frac{dU}{d\tau} + \left\{ \mathrm{Tr}\left(Q\frac{dQ}{d\tau}\right) B_1 + \mathrm{Tr}\left(Q^2\frac{dQ}{d\tau}\right) B_2 + f_1\frac{dQ}{d\tau} + f_2\frac{dQ}{d\tau}Q + f_2 Q\frac{dQ}{d\tau}\right\} U, \tag{71}$$

and hence,

$$\mathrm{Re\,Tr}\left(\Sigma'\frac{dU'}{d\tau}\right) = \mathrm{Re\,Tr}\left(\Sigma' e^{iQ}\frac{dU}{d\tau}\right) - \mathrm{Re\,Tr}\left(i\Lambda\frac{d\Omega}{d\tau}\right), \tag{72}$$

defining

$$\Lambda = \frac{1}{2}(\Gamma + \Gamma^\dagger) - \frac{1}{2N}\mathrm{Tr}(\Gamma + \Gamma^\dagger), \tag{73}$$

$$\Gamma = \mathrm{Tr}(\Sigma' B_1 U)Q + \mathrm{Tr}(\Sigma' B_2 U)Q^2 + f_1 U\Sigma' + f_2 QU\Sigma' + f_2 U\Sigma' Q. \tag{74}$$

One sees that $\Gamma_\mu^{(k-1)}(x)$, and hence, $\Lambda_\mu^{(k-1)}(x)$, are defined on each lattice link in terms of the link variables $U_\mu^{(k-1)}(x)$ and $\Sigma_\mu^{(k)}(x)$. At this point, the details of the staple construction in $C_\mu(x)$ must be included. Given Eq. (1) and utilizing trace cyclicity and translational invariance, one eventually obtains the following recursion relation:

$$\begin{aligned}\Sigma_\mu(x) = \Sigma'_\mu(x)(f_0 I + f_1 Q_\mu(x) + f_2 Q_\mu^2(x)) + iC_\mu^\dagger(x)\Lambda_\mu(x) - i\sum_{\nu\neq\mu}\{ &\rho_{\nu\mu}U_\nu(x+\hat\mu)U_\mu^\dagger(x+\hat\nu)U_\nu^\dagger(x)\Lambda_\nu(x) \\ &+ \rho_{\mu\nu}U_\nu^\dagger(x-\hat\nu+\hat\mu)U_\mu^\dagger(x-\hat\nu)\Lambda_\mu(x-\hat\nu)U_\nu(x-\hat\nu) + \rho_{\nu\mu}U_\nu^\dagger(x-\hat\nu+\hat\mu)\Lambda_\nu(x-\hat\nu+\hat\mu)U_\mu^\dagger(x-\hat\nu)U_\nu(x-\hat\nu) \\ &- \rho_{\nu\mu}U_\nu^\dagger(x-\hat\nu+\hat\mu)U_\mu^\dagger(x-\hat\nu)\Lambda_\nu(x-\hat\nu)U_\nu(x-\hat\nu) - \rho_{\nu\mu}\Lambda_\nu(x+\hat\mu)U_\nu(x+\hat\mu)U_\mu^\dagger(x+\hat\nu)U_\nu^\dagger(x) \\ &+ \rho_{\mu\nu}U_\nu(x+\hat\mu)U_\mu^\dagger(x+\hat\nu)\Lambda_\mu(x+\hat\nu)U_\nu^\dagger(x)\},\end{aligned} \tag{75}$$

in which unprimed quantities refer to step $(k-1)$ and primed quantities refer to step k.

Although the force field is related to the underlying link variables in a complicated manner, each step in the recursive computation of the force field outlined above is straightforward, facilitating a natural and efficient implementation in software. Analyticity in the entire (finite) complex plane is an important property here; if $\Sigma_\mu^{(k)}(x)$ is well behaved, then $\Sigma_\mu^{(0)}(x)$ must be also. Note that the above formalism can be easily adapted for other definitions of $C_\mu(x)$.

V. NUMERICAL TESTS

The efficacy of stout links both as a gluonic-operator smearing algorithm and for reducing the effects of ultraviolet gluon modes in short-distance quantities was tested in several Monte Carlo simulations.

The energy of gluons in the presence of a static quark-antiquark pair separated by a distance r can be extracted from $r\times t$ Wilson loops $W(r,t)$ as the temporal extent t becomes large. The Wilson loop can be viewed as the correlation function of a gauge-invariant operator consisting of a static quark-antiquark pair connected by a product of link variables following a straight-line path between the quark and the antiquark. Extraction of the lowest energy can be done much more reliably if the couplings of the quark-antiquark-gluon operator with higher-lying states are small. This can be achieved by utilizing a product of smeared links connecting the quark and the antiquark, instead of the original link variables. In other words, the ground state energy of gluons in the presence of a static quark-antiquark pair can be more reliably determined from Wilson loops $\widetilde{W}(r,t)$ constructed using smeared spatial links in the r-link paths on the initial and final time slices. A measure of how well the couplings to the higher levels are reduced is the effective energy for a single time step, defined by

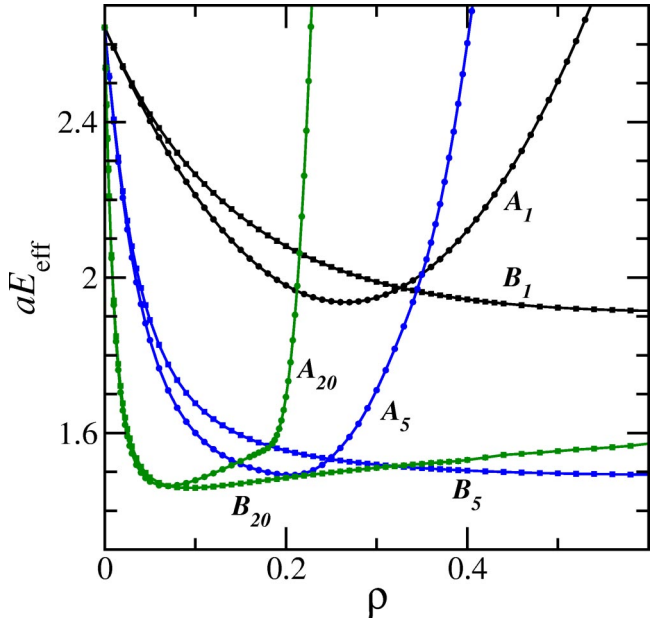

FIG. 2. The effective energy $aE_{\rm eff}(r)$ defined in Eq. (76) for a static quark-antiquark pair separated by a distance $r=5a$ for several levels of smearing $n_\rho=1$, 5, and 20 against the smearing parameter ρ. These results were obtained on a 12^4 lattice using the Wilson gauge action with coupling $\beta=5.7$. Curves labeled A_{n_ρ} indicate results using the spatially-isotropic three-dimensional version of the analytic stout link smearing scheme with $n_\rho=1$, 5, and 20 levels, while the curves labeled B_{n_ρ} show the results for links smeared using Eq. (12) with the projection method of Ref. [15].

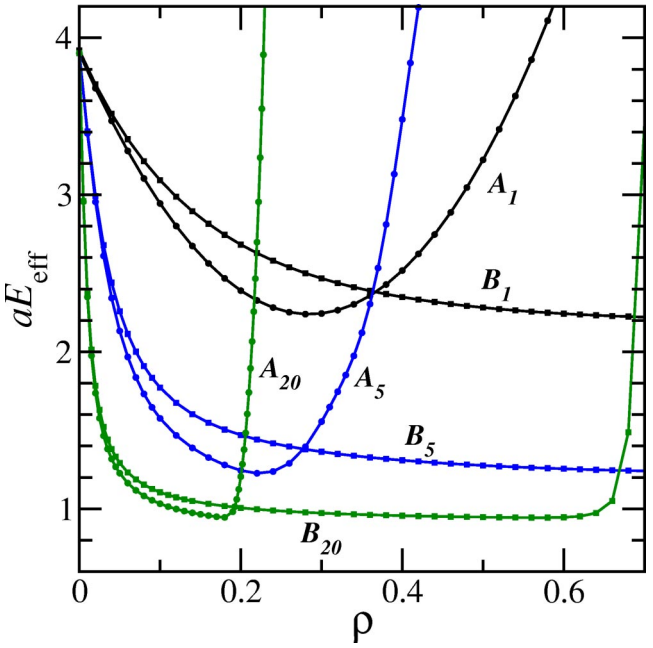

FIG. 3. The effective energy $aE_{\rm eff}(r)$ defined in Eq. (76) for a static quark-antiquark pair separated by a distance $r=10a$ for several levels of smearing $n_\rho=1$, 5, and 20 against the smearing parameter ρ. Results were obtained on a 24^4 lattice using the Wilson gauge action with coupling $\beta=6.2$. Curves labeled A_{n_ρ} indicate results using the spatially-isotropic three-dimensional version of the analytic stout link smearing scheme with $n_\rho=1$, 5, and 20 levels, while the curves labeled B_{n_ρ} show the results for links smeared using Eq. (12) with the projection method of Ref. [15].

$$aE_{\rm eff}(r)=-\ln\left(\frac{\tilde{W}(r,a)}{\tilde{W}(r,0)}\right). \tag{76}$$

Under unexceptional circumstances for a lattice gauge action with a positive-definite transfer matrix, such as the Wilson action, reducing the excited-state contamination tends to lower the effective energy given above.

The effective energy defined in Eq. (76) was used to test the ability of the stout link smearing scheme to reduce excited-state contamination in gluonic operators. Results for $r=5a$ on a 12^4 lattice using the Wilson gauge action with coupling $\beta=5.7$ are shown in Fig. 2, and results for $r=10a$ on a larger 24^4 lattice with $\beta=6.2$ are shown in Fig. 3. The results are compared to those obtained with links smeared using Eq. (12) and the projection method of Ref. [15].

Both figures show that link smearing can dramatically reduce contamination from the high-lying modes of the theory. Consider first the results obtained using the spatially-isotropic three-dimensional version of the stout link smearing scheme ($\rho_{jk}=\rho$, $\rho_{4\mu}=\rho_{\mu 4}=0$). For a given number of smearing iterations n_ρ, the effective energy decreases initially as the smearing parameter ρ is increased from zero. Eventually an optimal value for the smearing parameter is reached at which the effective energy is minimized. This optimal value decreases as the number of smearing levels n_ρ is increased, and the reduction in the effective energy at this optimal ρ value is substantial. Further increasing ρ beyond its optimal value then results in a sharply increasing effective energy. The rapidity of both the fall and rise of the effective energy about its minimum is more pronounced for larger n_ρ. Also, the minimum value decreases as n_ρ increases until eventually a saturation point is reached beyond which no additional reduction occurs.

The results obtained with links smeared using Eq. (12) and the projection method of Ref. [15] display essentially the same trends, except that each minimum in the effective energy is much broader. The increased sensitivity of the stout link smearing scheme to the parameter ρ is not surprising since ρ occurs inside an exponential function. However, it is important to note that both smearing methods produce nearly the same minimum values of the effective energy. The stout link smearing scheme is just as effective at reducing excited-state contamination in gluonic operators as the standard link fuzzing scheme in current use, although more careful tuning is necessary due to the increased sensitivity to the smearing parameter ρ. Note that this analytic link smearing method has already been successfully applied in computing the spectrum of torelon excitations [4].

The main purpose of using smeared links in lattice gauge and fermion actions is to reduce discretization effects caused by the ultraviolet modes in the lattice theory. Often such effects are dominated by large contributions from tadpole diagrams. A simple measure of how well a link smearing

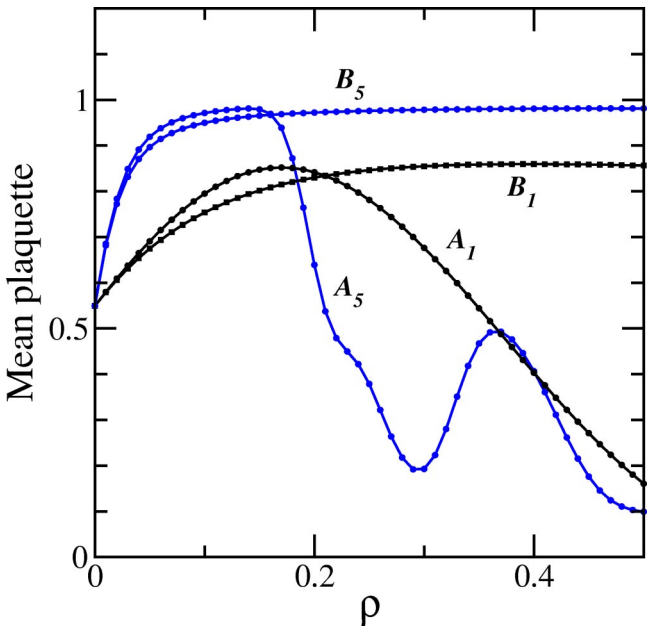

FIG. 4. The mean smeared plaquette against the smearing parameter ρ. These results were obtained using the Wilson gauge action on a 12^4 lattice with coupling $\beta=5.7$. Curves labeled A_{n_ρ} indicate results obtained using the isotropic four-dimensional version of the analytic stout link smearing scheme with $n_\rho=1$ and 5 levels, while the curves labeled B_{n_ρ} show the results with links smeared using Eq. (12) and the projection method of Ref. [15].

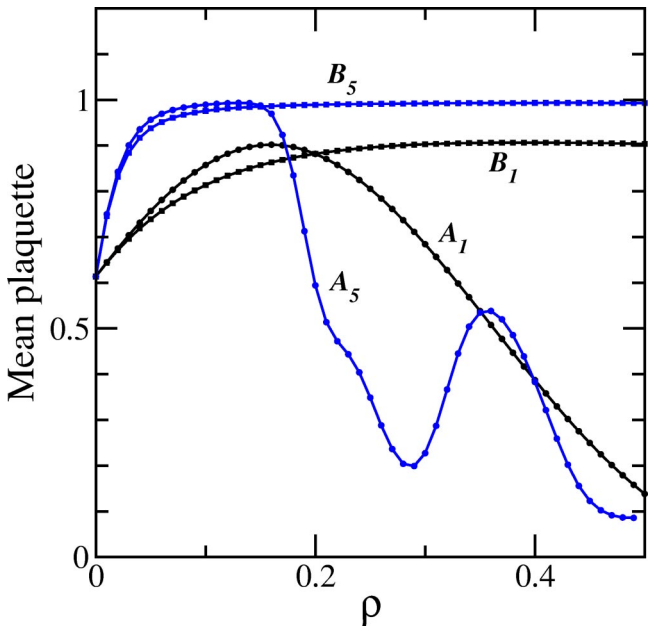

FIG. 5. The mean smeared plaquette against the smearing parameter ρ. These results were obtained using the Wilson gauge action on a 24^4 lattice with coupling $\beta=6.2$. Curves labeled A_{n_ρ} indicate results obtained using the isotropic four-dimensional version of the analytic stout link smearing scheme with $n_\rho=1$ and 5 levels, while the curves labeled B_{n_ρ} show the results with links smeared using Eq. (12) and the projection method of Ref. [15].

scheme can reduce artifacts from tadpole diagrams is the mean smeared plaquette, defined by

$$\tilde{P}=\frac{1}{18N_s}\sum_{x,\mu>\nu}\mathrm{Re\,Tr}\langle\tilde{U}_\mu(x)\tilde{U}_\nu(x+\hat{\mu})\tilde{U}^\dagger_\mu(x+\hat{\nu})\tilde{U}^\dagger_\nu(x)\rangle, \tag{77}$$

where N_s is the number of sites on the lattice. A value of the mean smeared plaquette near unity indicates a substantial reduction of the tadpole contributions.

Results for the mean smeared plaquette are shown for a 12^4 lattice using the Wilson gauge action with coupling $\beta=5.7$ in Fig. 4 and for a 24^4 lattice with coupling $\beta=6.2$ in Fig. 5. For isotropic four-dimensional versions ($\rho_{\mu\nu}=\rho$) of both smearing methods, the mean smeared plaquette initially increases towards unity as ρ increases from zero until a maximum is reached. The two smearing methods produce nearly the same maximum value. As ρ is increased further, the mean smeared plaquette in the stout link scheme quickly begins to fall, whereas the standard smearing scheme changes little. As n_ρ initially increases from zero, the maximum value of the mean plaquette also increases, but eventually a saturation point is reached. Note that the maximum values for $n_\rho=5$ are very near to unity, suggesting a dramatic reduction of tadpole contributions. A comparison of Figs. 4 and 5 shows a small sensitivity of the results with the coupling β. In summary, the analytic stout link smearing scheme is observed to be just as efficacious as the standard smearing scheme in reducing discretization effects from the ultraviolet gluon modes, but with an increased sensitivity to the smearing parameter ρ.

VI. CONCLUSION

Link-variable smoothing is a crucial ingredient in constructing gluonic operators which have dramatically reduced mixings with the high frequency modes of the theory. Link smearing is also playing an increasingly important role in the construction of improved lattice actions. The lack of differentiability with respect to the underlying link variables of standard smearing schemes prevents the use of efficient Monte Carlo updating methods based on molecular dynamics evolution.

A link smearing method which circumvents these problems was proposed and tested in this paper. The link smearing method is analytic everywhere in the finite complex plane and utilizes the exponential function in such a manner to remain within $SU(3)$, eliminating the need for any projection back into the group. Because of this construction, the algorithm is also useful for any Lie group. An efficient implementation of this smearing scheme, as well as the recursive computation of the force term describing the change of the action in response to a variation of the link variables, was described. Although the force field is related to the underlying link variables in a very complicated manner, each step in the recursive computation of the force field is actually

straightforward, allowing a natural and efficient design in software. The smeared mean plaquette and the effective energy associated with the static quark-antiquark potential were used to show that no degradation in effectiveness is observed as compared to link smearing methods currently in use, although an increased sensitivity to the smearing parameter was found.

ACKNOWLEDGMENTS

The authors wish to thank Robert Edwards and David Richards for helpful discussions. This work was supported by the U.S. National Science Foundation through grant PHY-0099450 and by Enterprise-Ireland Basic Research Grant SC/2001/306.

[1] C. Morningstar and M. Peardon, Phys. Rev. D **60**, 034509 (1999).
[2] P. Lacock, C. Michael, P. Boyle, and P. Rowland, Phys. Rev. D **54**, 6997 (1996).
[3] K. Juge, J. Kuti, and C. Morningstar, Phys. Rev. Lett. **82**, 4400 (1999).
[4] K. Juge, J. Kuti, F. Maresca, C. Morningstar, and M. Peardon, hep-lat/0309180.
[5] K. Juge, J. Kuti, and C. Morningstar, Phys. Rev. Lett. **90**, 161601 (2003).
[6] T. Blum *et al.* Phys. Rev. D **55**, 1133 (1997).
[7] T. DeGrand, Phys. Rev. D **58**, 094503 (1998).
[8] A. Hasenfratz and F. Knechtli, Phys. Rev. D **64**, 034504 (2001).
[9] G. Lepage, Phys. Rev. D **59**, 074502 (1999).
[10] K. Orginos and D. Toussaint, Phys. Rev. D **59**, 014501 (1999).
[11] K. Orginos, D. Toussaint, and R. Sugar, Phys. Rev. D **60**, 054503 (1999).
[12] J. Zanotti *et al.* Phys. Rev. D **65**, 074507 (2002).
[13] F. Niedermayer, P. Rufenacht, and U. Wenger, Nucl. Phys. **B597**, 413 (2001).
[14] M. Albanese *et al.* Phys. Lett. B **192**, 163 (1987).
[15] Y. Liang *et al.* Phys. Lett. B **307**, 375 (1993).
[16] S. Duane, A. Kennedy, B. Pendleton, and D. Roweth, Phys. Lett. B **195**, 216 (1987).
[17] Refers to their thick-bodied nature from the large brew of paths used in their formation (coined in a Dublin public house).
[18] M. Luscher and P. Weisz, Commun. Math. Phys. **97**, 59 (1985); **98**, 433(E) (1985).
[19] D. Callaway and A. Rahman, Phys. Rev. Lett. **49**, 613 (1982).
[20] J. Polonyi and H. Wyld, Phys. Rev. Lett. **51**, 2257 (1983); **52**, 401(E) (1984).
[21] S. Gottlieb, W. Liu, D. Toussaint, R. Renken, and R. Sugar, Phys. Rev. D **35**, 2531 (1987).
[22] W. Kamleh, D. Leinweber, and A. Williams, hep-lat/0309154.